

Journal of Materials Chemistry C

Accepted Manuscript



This is an *Accepted Manuscript*, which has been through the Royal Society of Chemistry peer review process and has been accepted for publication.

Accepted Manuscripts are published online shortly after acceptance, before technical editing, formatting and proof reading. Using this free service, authors can make their results available to the community, in citable form, before we publish the edited article. We will replace this *Accepted Manuscript* with the edited and formatted *Advance Article* as soon as it is available.

You can find more information about *Accepted Manuscripts* in the [Information for Authors](#).

Please note that technical editing may introduce minor changes to the text and/or graphics, which may alter content. The journal's standard [Terms & Conditions](#) and the [Ethical guidelines](#) still apply. In no event shall the Royal Society of Chemistry be held responsible for any errors or omissions in this *Accepted Manuscript* or any consequences arising from the use of any information it contains.

Cite this: DOI: 10.1039/c0xx00000x

COMMUNICATION

www.rsc.org/chemcomm

A new system for achieving high-quality nonpolar *m*-plane GaN-based light-emitting diode wafers

Wenliang Wang,^a Yunhao Lin,^a Weijia Yang,^a Zuolian Liu,^a Shizhong Zhou,^a Huirong Qian,^a Fangliang Gao,^a Lei Wen,^a Guoqiang Li^{a, b, *}

Received (in XXX, XXX) Xth XXXXXXXXX 20XX, Accepted Xth XXXXXXXXX 20XX
DOI: 10.1039/b000000x

High-quality nonpolar *m*-plane GaN-based light-emitting diode (LED) wafers have been deposited on the LiGaO₂(100) substrates by the combination of pulsed laser deposition and molecular beam epitaxy technologies. The high-resolution X-ray diffraction measurement reveals that high-crystalline quality nonpolar *m*-plane GaN films have been achieved on LiGaO₂(100) substrates. Scanning electron microscopy and atomic force microscopy reveal the very flat surface with a surface root-mean-square roughness of 1.3 nm for p-GaN in the nonpolar *m*-plane GaN-based LED wafer grown on LiGaO₂(100) substrates. A strong photoluminescence emission peak observed at 446 nm with a full width at half maximum (FWHM) of 21.2 nm. Meanwhile, the electroluminescence spectra of nonpolar *m*-plane GaN-based LEDs on LiGaO₂(100) substrates show a very slight blue shift in wavelength and is kept constant in FWHM with the increase of current from 20 to 150 mA. At an injection current of 20 mA, the light output power for this nonpolar LED is 30.1 mW and the forward voltage of 2.8 V in chip size of 300×300 μm². Furthermore, the nonpolar *m*-plane GaN-based LED on LiGaO₂(100) exhibits best external extraction efficiency value of 50.8%. These results indicate the high optoelectronic properties of nonpolar LEDs grown on LiGaO₂(100) substrates. This achievement of the nonpolar *m*-plane GaN-based LEDs on LiGaO₂(100) substrates brings up a new possibility for achieving highly-efficient LED devices.

Recently, III-nitrides such as AlN, GaN and InN, as well as their alloys have attracted remarkable considerations due to their inherent properties, which make them possible for the applications in light-emitting diodes (LEDs), laser diodes (LDs), and high electron mobility transistors (HEMTs), etc.¹⁻³ So far, *c*-plane GaN-based LEDs have already been successfully commercialized for a wide range of applications, such as general lighting, backlighting sources for liquid crystal display, and traffic signals.⁴⁻⁶ However, for these LEDs, one problem that has existed from the early days and is becoming enormously troublesome, is the large internal piezoelectric fields in the

multiple quantum wells (MQWs), which leads to the formation of quantum confined Stark effects (QCSEs). QCSEs can cause the separation of the holes and electrons wave functions in the quantum wells, and thereby reduce the radiative recombination efficiency ultimately.⁷⁻⁹ To overcome this problem, devices prepared on the nonpolar or semipolar orientation have been considered to be an effective approach to eliminate or reduce the piezoelectric fields, which can increase the internal quantum efficiency (IQE) of device to some extent.¹⁰⁻¹² So far, nonpolar GaN-based LEDs are usually grown on nonpolar sapphire or GaN substrates. However, the price for these two substrates are much expensive than LiGaO₂(100), which would increase the cost for the commercialization of the nonpolar *m*-plane GaN-based LEDs.

In our previous works,¹³⁻¹⁴ we have already proven that LiGaO₂(100) substrate is very suitable for the growth of high-quality nonpolar *m*-plane GaN-based LEDs owing to the small lattice and thermal expansion mismatches between LiGaO₂(100) and GaN(1-100). Ever since, much effort has been made to realize the growth of high-quality nonpolar *m*-plane GaN-based LED wafers on LiGaO₂(100) substrates based on our previous work.

In this work, we report on the deposition of nonpolar *m*-plane GaN-based LED wafers on LiGaO₂(100) substrates by the combination of pulsed laser deposition (PLD) and molecular beam epitaxy (MBE) technologies for the first time. Detailed studies using high-resolution X-ray diffraction (HRXRD), scanning electron microscopy (SEM), atomic force microscopy (AFM), Hall measurement, photoluminescence (PL), and electroluminescence (EL) reveal the high structural properties, surface morphologies, and optoelectronic properties of as-grown nonpolar *m*-plane GaN-based LED wafers on LiGaO₂(100) substrates.

In this work, the GaN-based LED wafers were grown in the ultra-high vacuum (UHV) load-lock chamber at a background pressure of 1.0×10⁻⁸ Torr, where PLD was attached to the MBE chamber. A 50 nm thick *m*-plane GaN buffer layer with a full width at half maximum (FWHM) of 0.55° from its XRD rocking curve was firstly grown on LiGaO₂ substrate at a temperature as low as 200 °C by PLD. Secondly, a 300 nm thick higher-quality

m-plane GaN with an FWHM of 0.14° was then grown on this template by MBE at 500°C . Subsequently, a $3\ \mu\text{m}$ thick *m*-plane GaN layer was grown by MBE at 750°C to further enhance the crystalline quality of *m*-plane GaN, ending up with an FWHM of 0.090° from its GaN(1-100) XRD rocking curve. During the growth of the above layers, X-ray photoelectron spectroscopy (XPS) was deployed to monitor the surface concentration of each layer, and no trace of Li was detected, indicating that the initial low-temperature *m*-plane GaN buffer layer had effectively suppressed the Li diffusion from the substrate. A $4\ \mu\text{m}$ thick Si-doped *m*-plane GaN layer was then grown by MBE at 750°C . Afterwards, 7 periods InGaN (3 nm)/GaN (12 nm) MQWs were grown by MBE at 700°C , followed by a 20 nm thick AlGaIn layer acting as electron barrier layer. Finally, a 300 nm thick Mg-doped p-GaN layer was grown at 700°C on the top. The specialized electrochemical measurement systems called electrochemical quartz crystal microbalances (EQCMs) was utilized in the MBE system to monitor the thickness of as-grown films.¹⁵⁻¹⁶ During the whole process, *in-situ* reflection high energy electron diffraction (RHEED) was adopted to monitor the growth conditions. In order to investigate how the LiGaO₂ substrate affects the performance of LEDs, another LED wafer with the identical structure grown on *c*-plane sapphire substrate under the same growth conditions was prepared. Fig. 1a shows the structure of the nonpolar *m*-plane GaN-based LED wafers grown on LiGaO₂(100) substrates.

Fig. 1b illustrates the structure of the nonpolar *m*-plane GaN-based LED chips. The as-grown LED wafers were made into chips with the standard processes. First, the as-grown LEDs were cleaned by acetone and deionized water in turns. Subsequently, an inductively coupled plasma reactive ion etching (ICP-RIE) system was utilized to partially etch the p-GaN layer until the n-type GaN layer was exposed for n-type Ohmic contact. Afterwards, the p-GaN layer was activated at 700°C in N₂ atmosphere for 30 min in order to partially repair the damage induced by dry etching. A 250 nm-thick indium-tin oxide (ITO) layer was then deposited on the p-GaN layer by an electronic beam evaporator, followed by the deposition of Cr/Pt/Au (50/150/2000 nm) metals as n- and p-electrodes in a N₂ atmosphere at 500 and 380°C , respectively. Then, the samples were subjected to rapid thermal annealing for 1 min at the temperature of 700°C in N₂ atmosphere to enhance the Ohmic contact. Finally, the wafers were divided into individual chips with sizes of $300\times 300\ \mu\text{m}^2$. To determine the specific contact resistance ρ_c , current-voltage (I-V) measurements on several transmission line model (TLM) patterns were carried out by using the Karl Suss Microtec probe station equipped with a HP 4156B parameter analyzer at RT, and the spacings between the pads were 3, 4.5, 6, 7.5, 9, and $10\ \mu\text{m}$.

The as-grown GaN-based LED wafers were characterized by HRXRD (Bruker D8 X-ray diffractometer with Cu *K* α X-ray source, $\lambda=0.15406\ \text{nm}$) for structural properties, and by SEM (Nova NanoSEM 430 Holland) and AFM (MFP-3D-S Asylum American) for surface morphologies. The optical properties of MQWs were studied by 405 nm laser (YWafer GS4-GaN-R-405) with an output power of 20 mW at room temperature (RT). The optoelectronic properties of GaN-based LEDs were investigated using the GAMMA Scientific GS-1190 RadoMA-Lite KEITHLEY 2400 system and the Swin Hall 8800 system.

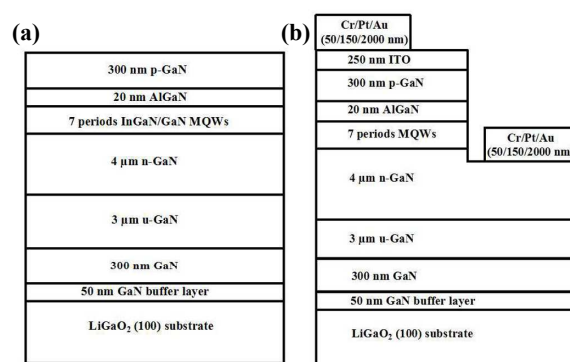


Fig. 1. Schematic structures of (a) GaN-based LED wafer grown on LiGaO₂(100) substrate, and (b) its chip.

The surface morphologies of GaN-based LEDs grown on LiGaO₂(100) and *c*-plane sapphire are studied by SEM and AFM, as shown in Fig. 2a-d. Pits and black spots can be noticed both in the Fig. 2a and b. However, the pits and black spots for p-GaN on *c*-plane sapphire substrates are much more than that on LiGaO₂(100) substrates. We attribute these differences to the higher Mg-doping efficiency in nonpolar *m*-plane p-GaN layers due to its higher hole concentration.¹⁷⁻¹⁹ The poorer Mg-doping efficiency in p-GaN grown on *c*-plane sapphire would introduce much more defects, such as pits and black spots. In this case, the surface morphologies for p-GaN grown on *c*-plane sapphire substrates are much worse than that on LiGaO₂(100) substrates. Meanwhile, the AFM measurement has revealed that the surface root-mean-square roughness for nonpolar p-GaN and *c*-plane p-GaN are 1.3 and 2.7 nm, as shown in Figs. 2c and d, which is consistent well with the SEM measurement.

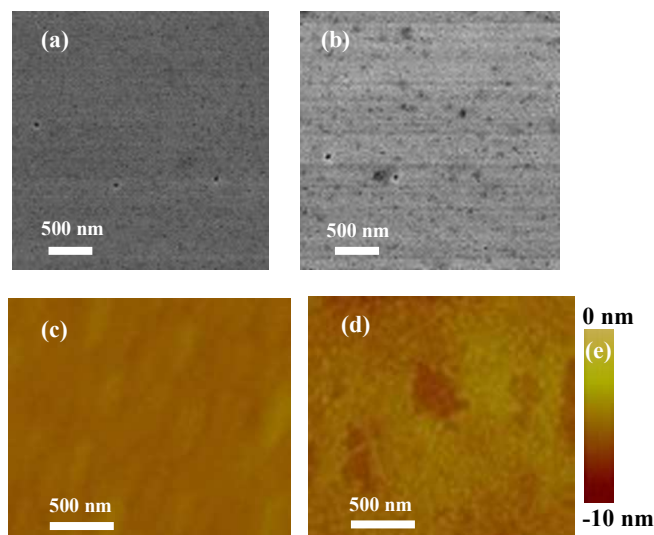


Fig. 2. SEM images for GaN-based LEDs grown on (a) LiGaO₂(100), and (b) *c*-plane sapphire substrates. AFM images for GaN-based LEDs grown on (c) LiGaO₂(100), and (d) *c*-plane sapphire substrates. (e) is the colour scale of AFM images.

The carrier mobility and concentration for the GaN-based LED wafers grown on LiGaO₂(100) and *c*-plane sapphire substrates are studied by conventional van der Pauw Hall measurement at RT. As for the nonpolar *m*-plane GaN-based LED wafers, the Si-doped n-GaN layers have an electron mobility and an electron concentration of $330\ \text{cm}^2/\text{Vs}$ and $5.9\times 10^{18}\ \text{cm}^{-3}$, respectively; and the Mg-doped GaN layers have a hole mobility and a hole concentration of $12.5\ \text{cm}^2/\text{Vs}$ and $2.8\times 10^{18}\ \text{cm}^{-3}$, respectively.

But for the GaN-based LED wafers grown on *c*-plane sapphire substrates, the Si-doped n-GaN layers have an electron Hall mobility and an electron concentration of 315 cm²/Vs and 4.0×10¹⁸ cm⁻³, respectively; and the Mg-doped GaN layers have a hole mobility and a hole concentration of 9.5 cm²/Vs and 4.9×10¹⁷ cm⁻³, respectively. Therefore, the electronic properties for GaN-based LED wafers grown on LiGaO₂(100) substrates are much better than that on *c*-plane sapphire substrates due to its higher hole mobility and concentration, and is beneficial to the radiative recombination of carriers in nonpolar *m*-plane GaN-based LED on LiGaO₂(100) substrate.^{17, 20-21}

The optical properties of as-grown non-polar *m*-plane InGaN/GaN MQWs are studied by PL at RT, as shown in Fig. 3. It can be noted that a sharper and stronger PL peak is observed at 446 nm with an FWHM of 21.2 nm for the nonpolar *m*-plane GaN-based LED on LiGaO₂(100) substrate when compared with that grown on *c*-plane sapphire substrate with an FWHM of 23.5 nm. Meanwhile, this PL FWHM is much smaller than that of the cubic InGaN/GaN MQWs grown on 3C-SiC(001).²² This achievement of high-quality MQWs on LiGaO₂(100) substrate can be tentatively attributed to two aspects. One is the adoption of the LiGaO₂(100) substrate, and the other is the combination of PLD and MBE technologies. The former provides smaller lattice and thermal expansion mismatches between GaN and LiGaO₂(100) compared with that between GaN and *c*-plane sapphire substrate, which is beneficial to the nucleation of GaN and shows a reduction in the formation of threading dislocations.¹³⁻¹⁴ Furthermore, it can achieve nonpolar *m*-plane GaN-based LED with the absence of the QCSEs, which can promote the radiative recombination of holes and electrons and further enhance the IQE when compared with the GaN-based LED on *c*-plane sapphire substrate.¹¹⁻¹² The latter can effectively suppress the diffusion of Li atoms from the substrate by using PLD growth of GaN buffer layer at low temperature.¹³⁻¹⁴ Meanwhile, it is good for us to achieve high-quality nonpolar *m*-plane GaN films by using MBE growth with high temperature and finally to realize the growth of high-quality nonpolar *m*-plane InGaN/GaN MQWs.

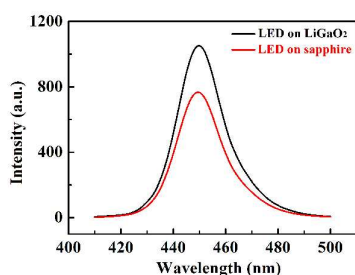


Fig. 3. RT PL for the InGaN/GaN MQWs on LiGaO₂(100) and *c*-plane sapphire substrates

Fig. 4a is the EL spectra of non-polar *m*-plane GaN-based LED grown on LiGaO₂(100) substrate under various currents at RT. We can clearly observe that there is a slight blue shift in wavelength with the increase in current from 20 to 150 mA as shown in Fig. 4a, which is strictly different from the GaN-based LED on *c*-plane sapphire substrate and is consistent with the results reported by S. Nakamura.^{5-6, 23} This slight blue shift in wavelength can be explained by the band filling of the localized states induced by the fluctuation of In composition in InGaN quantum wells.¹⁹ Meanwhile, the dependence of FWHMs on injection current for GaN-based LEDs grown on LiGaO₂(100)

and *c*-plane sapphire substrates is shown in Fig. 4b. It can be found that as the increase in current, the EL FWHM for GaN-based LED on *c*-plane sapphire substrate gradually increases, while that for GaN-based LED grown on LiGaO₂(100) substrate keeps constant. This can be ascribed to the absence of QCSEs and the slight band filling effect in MQWs on LiGaO₂(100) with the increase in current.^{11-12, 24-26} It is known to us that due to the In composition inhomogeneity and monolayer thickness fluctuation in the InGaN wells, self-organized In-rich area may be generated in InGaN active area, leading to the fluctuation of energy band-gap ultimately.²⁴⁻²⁷ Furthermore, this EL FWHM obtained in nonpolar *m*-plane GaN-based LED on LiGaO₂(100) substrate is much smaller than that of semipolar or nonpolar GaN-based LED on sapphire and nonpolar *m*-plane GaN-based LED on LiAlO₂(100) substrate,^{5-6, 22, 24} which may be ascribed to the smaller lattice and thermal expansion mismatches between GaN films and LiGaO₂(100) substrates when compared with that between GaN and semipolar sapphire or LiAlO₂(100) substrates.

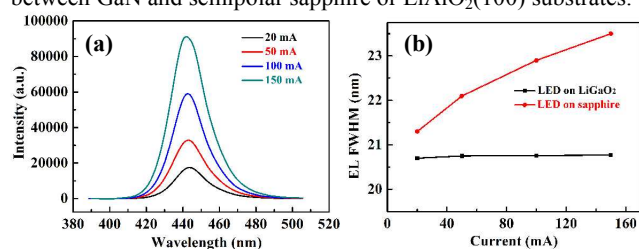


Fig. 4. (a) RT EL of nonpolar *m*-plane GaN-based LEDs grown on LiGaO₂(100) substrates with various currents, and (b) the dependence of FWHM on current for GaN-based LEDs grown on LiGaO₂(100) and *c*-plane sapphire substrates

The specific contact resistances ρ_s and contact resistances R_c are determined by transmission line model (TLM) characterization, which is reported in Fig. 5a. After careful study on the different TLM patterns using the linear square method to fit the straight lines to the experimental data, the specific contact resistances ρ_s for the contacts on the p-GaN layers grown on the LiGaO₂(100) and *c*-plane sapphire substrates are obtained with values of approximately 4.5×10⁻⁵ and 3.8×10⁻⁴ Ω·cm², and the contact resistances R_c for these two contacts are ~ 2.1 and 5.6 Ω·mm, respectively.²⁸⁻³² These results reveal the better Ohmic contact between nonpolar *m*-plane p-GaN and p-electrodes. We ascribe it to the higher hole concentration in nonpolar *m*-plane p-GaN layer.²⁸⁻³¹ Furthermore, using the same method, the specific contact resistances ρ_s for the n-GaN layer grown on the LiGaO₂(100) and *c*-plane sapphire substrates are about 9.4×10⁻⁶ and 6.5×10⁻⁵ Ω·cm², and the contact resistances R_c for these two contacts are 0.5 and 1.5 Ω·mm, respectively. Fig. 5b is the light output power (L) as a function of current (I) for LED chips on both LiGaO₂(100) and *c*-plane sapphire substrates. It can be easily noted that the light output power values for both samples increase monotonously with the increase in current. Moreover, it also can be found the light output power for LED chip on LiGaO₂(100) substrate is higher than that on *c*-plane sapphire substrate. For example, at current injection of 20 mA, the output power values for LED chips on LiGaO₂(100) and *c*-plane sapphire are 30.1 and 19.2 mW, respectively. Meanwhile, this value of LED chip on LiGaO₂(100) is comparable to the best values ever reported for semipolar or nonpolar LEDs.^{6, 33} This

great improvement in light output power is mainly attributed to the uniformity of current spreading in the LED chip on LiGaO₂(100) due to the absence of the QCSEs in MQWs on LiGaO₂(100) substrate, which enhances the IQE and external extraction efficiency (EQE).³⁴⁻³⁶ Fig. 5c shows the relationship between forward voltage and injection current for LED chips grown on LiGaO₂(100) and *c*-plane sapphire substrates. The forward voltage measured at 20 mA for LED chip grown on LiGaO₂(100) and *c*-plane sapphire substrates are 2.8 and 3.1 V, respectively. We attribute the lower forward voltage for LED chip grown on LiGaO₂(100) substrate to the lower series resistance in LED chip on LiGaO₂(100) substrate of $\sim 7 \Omega$ compared with that on *c*-plane sapphire substrate of $\sim 10 \Omega$.^{4, 37-42} Furthermore, the EQE for LED chips on LiGaO₂(100) and *c*-plane sapphire substrates are also be studied. Fig. 5d illustrates the EQE of the nonpolar *m*-plane GaN-based LED chip grown on LiGaO₂(100) versus current density in the comparison with the LED chip grown on *c*-plane sapphire substrate. One can clearly identify the dramatic decrease in EQE for LED chip grown *c*-plane sapphire substrate as the increase in the current density; while the EQE for LED chip on LiGaO₂(100) substrate decreases much more slowly, and with a relatively high value of 41% even at the current density of 200 A/cm². This may be attributed to the absence of the QCSEs in LED chip grown on LiGaO₂(100) substrate. Moreover, the best value of EQE for LED chip on LiGaO₂(100) is 50.8%, which is comparable with the reported value of semipolar GaN-based LED chip grown on bulk GaN substrate,^{4-6, 41} and is much better than the commercial available LED chip with the EQE of about 30%.^{23, 41}

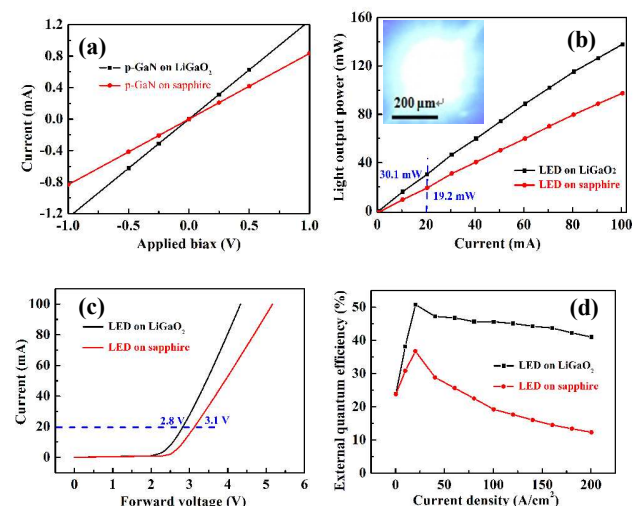


Fig. 5. (a) The I-V characteristics of Cr/Pt/Au contacts on the p-GaN grown on LiGaO₂(100) and *c*-plane sapphire substrates, respectively, measured over Ohmic pads with a spacing of 3 μm. (b) L-I, (c) I-V, and (d) EQE-I characteristics of GaN-based LED chips with the size of 300×300 μm² on both LiGaO₂(100) and *c*-plane sapphire substrates. The inset photograph in Fig. 5b is a lit-up LED on LiGaO₂(100) substrate working at an injection current of 20 mA.

To summarize, high-quality nonpolar *m*-plane GaN-based LED wafers have been deposited on the LiGaO₂(100) and *c*-plane sapphire substrates by the combination of PLD and MBE technologies. The as-grown GaN-based LED wafers have been

characterized by HRXRD, SEM, AFM, Hall, PL and EL measurement. The SEM and AFM measurements reveal the much flatter surface for p-GaN layers on the nonpolar *m*-plane GaN-based LED on the LiGaO₂(100) compared with that on *c*-plane sapphire substrates. The Hall measurement indicates the higher hole mobility and concentration, and is beneficial to the radiative recombination of carriers. The PL of as-grown nonpolar *m*-plane GaN-based LED wafers on LiGaO₂(100) substrates shows an emission peak at 446 nm with a smaller FWHM of 21.2 nm when compared with that on *c*-plane sapphire substrate of 23.5 nm. Meanwhile, the EL spectra of nonpolar *m*-plane GaN-based LEDs on LiGaO₂(100) substrates show a very slight blue shift in wavelength and is kept constant in FWHM, indicating that high-quality nonpolar *m*-plane GaN-based LEDs on LiGaO₂(100) have been achieved. LED chips with the size of 300×300 μm² prepared on LiGaO₂(100) substrates show a light output power of 30.1 mW and a forward voltage of 2.8 V at an injection of 20 mA, which is a dramatic contrast to the 19.2 mW and 3.1 V for the identical LED chips on *c*-plane sapphire substrates. Furthermore, the nonpolar *m*-plane GaN-based LED on LiGaO₂(100) shows a best EQE of 50.8%, which is comparable with the best value ever reported for semipolar or nonpolar GaN-based LEDs. Evidently, we have prepared high-quality nonpolar *m*-plane GaN-based LEDs on LiGaO₂(100) substrates, which brings up a new possibility for achieving highly-efficient LEDs. In addition, we have also proposed and demonstrated that the methodology by the combination of PLD and MBE is an effective approach to achieve high-quality nonpolar *m*-plane GaN-based LEDs on LiGaO₂(100) substrates. This methodology also sheds light on the application of other chemically vulnerable substrates for the fabrication of LEDs.

This work is supported by National Natural Science Foundation of China (Nos. 51002052, and 51372001), Key Project in Science and Technology of Guangdong Province (No. 2011A080801018), Excellent Youth Foundation of Guangdong Scientific Committee (No. S2013050013882), and Strategic Special Funds for LEDs of Guangdong Province (Nos. 2011A081301010, and 2011A081301012). Wenliang Wang and Yunhao Lin contribute equally to this work.

Notes and references

- ^a State Key Laboratory of Luminescent Materials and Devices, South China University of Technology, Guangzhou 510641, China
^b Department of Electronic Materials, South China University of Technology, Guangzhou 510641, China
^{*} Corresponding E-mail: msgli@scut.edu.cn
[†] Electronic Supplementary Information (ESI) available. See DOI: 10.1039/b000000x/

- 1 P. Waltereit, O. Brandt, A. Trampert, H. T. Grahn, J. Menniger, M. Ramsteiner, M. Reiche and K. H. Ploog, *Nature*, 2000, **406**, 865-868.
- 2 Y. Kobayashi, K. Kumakura, T. Akasaka and T. Makimoto, *Nature*, 2012, **484**, 223-227.
- 3 W. L. Wang, H. Yang and G. Q. Li, *J. Mater. Chem. C*, 2013, **1**, 4070-4077.
- 4 C. Y. Cho, N. Y. Kim, J. W. Kang, Y. C. Leem, S. H. Hong, W. Lim, S. T. Kim and S. J. Park, *Appl. Phys. Express*, 2013, **6**, 042102.
- 5 Y. J. Zhao, S. H. Oh, F. Wu, Y. Kawaguchi, S. Tanaka, K. Fujito, J. S. Speck, S. P. DenBaars and S. Nakamura, *Appl. Phys. Express*, 2013, **6**, 062102.
- 6 Y. J. Zhao, S. Tanaka, C. C. Pan, K. Fujito, D. Feezell, J. S. Speck, S. P. DenBaars and S. Nakamura, *Appl. Phys. Express*, 2013, **6**, 082104.

- 7 M. N. Islam, C. E. Soccolich, R. E. Slusher, A. F. J. Levi, W. S. Hobson and M. G. Young, *J. Appl. Phys.*, 1992, **71**, 1927-1935.
- 8 P. K. Basu and S. K. Paul, *J. Appl. Phys.*, 1992, **71**, 3617-3619.
- 9 S. Chichibu, T. Azuhata, T. Sota and S. Nakamura, *Appl. Phys. Lett.*, 1996, **69**, 4188-4190.
- 10 D. F. Feezell, J. S. Speck, S. P. DenBaars and S. Nakamura, *J. Disp. Technol.*, 2013, **9**, 190-198.
- 11 F. Scholz, *Semicond. Sci. Technol.*, 2012, **27**, 024002.
- 12 H. Masui, S. Nakamura, S. P. DenBaars and U. K. Mishra, *IEEE T. Electron. Dev.*, 2010, **57**, 88-100.
- 13 G. Q. Li, S. Shih and Z. Fu, *Chem. Commun.*, 2010, **46**, 1206-1208.
- 14 W. J. Yang, W. L. Wang, Y. H. Lin, Z. L. Liu, S. Z. Zhou, H. R. Qian, S. G. Zhang and G. Q. Li, *J. Mater. Chem. C*, 2014, **2**, 801-805.
- 15 X. Xu, Y. Du and S. M. George, *J. Vac. Sci. Technol. A*, 2005, **23**(4), 581-588.
- 16 T. R. Itzdorf, Modern Electroplating, Fifth Edition, Edited by Mordechai Schlesinger and Milan Paunovic. *John Wiley & Sons, Inc.* 2010.
- 17 M. McLaurin, T. E. Mates and J. S. Speck, *Appl. Phys. Lett.*, 2005, **86**, 262104.
- 18 Y. J. Sun, O. Brandt, S. Cronenberg, H. T. Grahn and K. H. Ploog, *Phys. Stat. Sol. b*, 2003, **240**, 360-363.
- 19 J. J. Wierer, A. David and M. M. Megens, *Nature Photon.*, 2009, **3**, 163-169.
- 20 Y. Taniyasu, J. F. Carlin, A. Castiglia, R. Butté, N. Grandjean, *Appl. Phys. Lett.*, 2012, **101**, 082113.
- 21 K. M. Song, J. M. Kim, B. K. Kang, D. H. Yoon, S. Kang, S. W. Lee, S. N. Lee, *Appl. Phys. Lett.*, 2012, **100**, 212103.
- 22 S. F. Li, J. Schörmann, D. J. As and K. Lischka, *Appl. Phys. Lett.*, 2007, **90**, 071903.
- 23 S. Nakamura, *MRS Bull.*, 2009, **34**, 101-107.
- 24 B. Liu, R. Zhang, Z. L. Xie, C. X. Liu, J. Y. Kong, J. Yao, Q. J. Liu, Z. Zhang, D. Y. Fu, X. Q. Xiu, H. Lu, P. Chen, P. Han, S. L. Gu, Y. Shi and Y. D. Zheng, *Appl. Phys. Lett.*, 2007, **91**, 253506.
- 25 S. Chichibu, T. Sota, K. Wada and S. Nakamura, *J. Vac. Sci. Technol. B*, 1998, **16**, 2204-2214.
- 26 T. Wang, D. Nakagawa, J. Wang, T. Sugahara and S. Sakai, *Appl. Phys. Lett.*, 2007, **73**, 3571-3573.
- 27 T. Kuroda and A. Tackeuchi, *J. Appl. Phys.*, 2002, **92**, 3071-3074.
- 28 S. C. Han, J. K. Kim, J. Y. Kim, D. M. Lee, J. S. Yoon, J. K. Kim, E. F. Schubert and J. M. Lee, *J. Nanosci. Nanotechnol.*, 2013, **13**, 5715-5718.
- 29 M. S. Oh, D. K. Hwang, J. H. Lim, C. G. Kang, and S. J. Park, *Appl. Phys. Lett.*, 2016, **89**, 042107.
- 30 H. J. Li and Y. Shi, *Semicond. Technol.*, 2008, **33**, 155-159.
- 31 G. Greco, P. Prystawko, M. Leszczyski, R. Lo Nigro, V. Raineri and F. Roccaforte, *J. Appl. Phys.*, 2011, **110**, 123703.
- 32 D. Qiao, L. Jia, L. S. Yu, P. M. Asbeck, S. S. Lau, S.-H. Lim, Z. Liliental-Weber, T. E. Haynes and J. B. Barner, *J. Appl. Phys.*, 2001, **89**, 5543-5546.
- 33 Y. Zhao, J. Sonoda, C. C. Pan, S. Brinkley, I. Koslow, K. Fujito, H. Ohta, S. P. DenBaars and S. Nakamura, *Appl. Phys. Express*, 2010, **3**, 102101.
- 34 Y. J. Lee, C. H. Chiu, C. C. Ke, P. C. Lin, T. C. Lu, H. C. Kuo and S. C. Wang, *IEEE J. Sel. Top. Quantum Electron.*, 2009, **15**, 1137-1143.
- 35 J. Y. Zhang, L. E. Cai, B. P. Zhang, X. L. Hu, F. Jiang, J. Z. Yu and Q. M. Wang, *Appl. Phys. Lett.*, 2009, **95**, 161110.
- 36 L. H. Peng, C. W. Chuang and L. H. Lou, *Appl. Phys. Lett.*, 1999, **74**, 795-797.
- 37 J. K. Sheu, S. J. Tu, Y. H. Yeh, M. L. Lee and W. C. Lai, *Appl. Phys. Lett.*, 2012, **101**, 151103.
- 38 T. F. Chen, Y. Q. Wang, P. Xiang, R. H. Luo, M. G. Liu, W. M. Yang, Y. Ren, Z. Y. He, Y. B. Yang, W. J. Chen, X. R. Zhang, Z. S. Wu, Y. Liu and B. J. Zhang, *Appl. Phys. Lett.*, 2012, **100**, 241112.
- 39 L. Liu and J. H. Edgar, *Mater. Sci. Eng. R*, 2002, **37**, 61-127.
- 40 Y. J. Sun, T. J. Yu, C. Y. Jia, Z. Z. Chen, P. F. Tian, X. N. Kang, G. J. Lian and G. Y. Zhang, *Chin. Phys. Lett.*, 2012, **27**, 127303.
- 41 S. P. DenBaars, D. Feezell, K. Kelchner, S. Pimpitkar, C. C. Pan, C. C. Yen, S. Tanaka, Y. J. Zhao, N. Pfaff, R. Farrell, M. Iza, S. Keller, U. Mishra, J. S. Speck and S. Nakamura, *Acta Materialia*. 2013, **61** 945-951.
- 42 B. H Kong, W. S. Han, H. K. Cho, M. Y. Kim, R. J. Choi and B. K. Kim, *J. Cryst. Growth*, 2008, **310**, 4916-4919.